Arkadiusz MIASKOWSKI[1], Andrzej WAC-WŁODARCZYK[2], Grażyna OLCHOWIK[3]

University of Life Sciences in Lublin (1), Lublin University of Technology (2), Medical University of Lublin (3)

Low Frequency FDTD Algorithm and its Application to Inductive Hyperthermia

Abstract. *The paper attempts to show the application of low frequency FDTD algorithm to the investigation of ACD and SAR distribution in female breast phantom and their dependence on frequency. Special attention has been given to the values of ACD and SAR in the skin layer because both of them play an important role in hyperthermia treatment when skin overheating occurs.*

Streszczenie. *W artykule przedstawiono zastosowanie algorytmu niskoczęstotliwościowego FDTD do analizy gęstości prądów wirowych i SAR w modelu gruczołu piersiowego. Szczególną uwagę położono na wartość wspomnianych wielkości w warstwie skóry ze względu na efekt jej przegrzania, jaki ma miejsce podczas leczenia hipertermicznego* ***(Zastosowanie niskoczęstotliwościowego algorytmu FDTD w hipertermii indukcyjnej.)****.*

Keywords: please : hyperthermia, FDTD, eddy currents, SAR.
Słowa kluczowe: hipertermia, FDTD, gęstość prądów wirowych, SAR.

Introduction

The power of healing by heat generation has been known for a long time. It is known as an innovative form of cancer therapy among classical methods like chemotherapy, surgery and irradiation. In general, hyperthermia is based on the principle that temperatures higher than 42^0C may lead to apoptosis. Apart from clinical problems, theoretical and engineering tasks have to be solved. One of them is the proper design of hyperthermia applicators in order get the required temperature distribution inside a cancer [1] or to avoid the skin overheating during treatment in inductive hyperthermia. The main challenge during the development of such devices, is the detailed understanding of the field distribution inside the body, since measurement inside living organisms is almost impossible. More over, in times of growing product complexity and shorter development cycles simulations are an essential part of a development process. These help the engineer to analyze a large number of variants of a design within a short time without building up prototypes for each design alternative. Here, simulation can be of great benefit. In this paper the authors have not considered temperature distribution on the skin but investigated two factors that are responsible for heat generation in a human body i.e. alternative current density (ACD) and Specific Absorption Rate (SAR). Both of them have to be considered when hyperthermia applicators are designed in order to avoid impedance mismatches on skin-applicator interface.

Low frequency FDTD algorithm

The finite-difference time-domain technique is a well established numerical method for modelling very complicated, inhomogeneous electromagnetic problems at high frequencies [2,3]. However, bioelectromagnetic simulations at low frequencies using FDTD method require special consideration [4]. Frequency scaling algorithm is often used at quasi-static frequencies, where the E-field and H-field are assumed to be uncoupled. Using this algorithm the actual simulation is performed at a higher frequency (f*) (with the quasi-static approximation being still valid) and the induced fields are scaled to the frequency of interest (f) after the higher frequency FDTD-simulation is finished. Assuming that the electric field in the air (E_{air}) is normal to the body surface, one can write:

$$j\omega\varepsilon_0\hat{n}E_{air}(\omega)=(\sigma+j\omega\varepsilon)\hat{n}E_{tissue}(\omega) \tag{1}$$

From (1) it can be concluded that:

$$E_{tissue}(\omega)=\frac{\omega\left(\sigma^*+j\omega^*\varepsilon^*\right)}{\omega^*(\sigma+j\omega\varepsilon)}E_{tissue}\left(\omega^*\right)\cong\frac{f\sigma^*}{f^*\sigma}E^*{}_{tissue}\left(f^*\right) \tag{2}$$

Assuming that $\sigma+j\omega\varepsilon\cong\sigma$ for both f and f* and σ^* and σ are close enough, the equation (2) can be simplified to:

$$E_{tissue}(f)=\frac{f}{f^*}E^*_{tissue}\left(f^*\right) \tag{3}$$

In our case the actual FDTD calculations were performed at the frequency f^* = 10 MHz and afterwards the induced electric field E^* at the frequency f^* was scaled to the frequency of question, i.e. f =150 Hz, using equation (3). As it is obvious from (2), the permittivity of tissues doesn't affect the results significantly, therefore the value of ε_r = 1 was set for the whole environment to hasten the speed of wave propagation and to reduce the simulation time. On the surface of the simulation, volume absorbing boundary conditions were defined. In this study, Berenger's [5] six perfectly matched layers (PML) boundary condition was used because it is superior to most standard absorbing boundary conditions (ABC) with regard to electromagnetic interferences with human tissues.

In order to validate the low frequency FDTD algorithm a model of disk has been prepared as shown in Fig. 1.

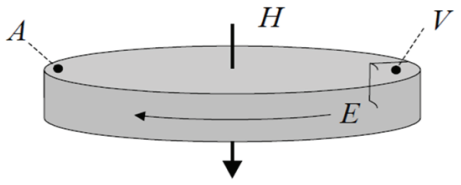

Fig. 1. The model of disk

The following parameters have been assigned to the disk: r_0 = 15cm, σ = 0.23 S/m, ε_r = 1, ρ =1 g/cm^3, H = 1 A/m, f = 50 Hz. *H*-field induce circulating CD in the disk i.e.

$$E(r)=\pi fr\mu_0 H \tag{4}$$

$$J(r)=\sigma E(r) \tag{5}$$

$$SAR=\sigma\frac{E^2(r)}{\rho} \tag{6}$$

Taking into account the parameters of the disk (Fig.1) one can calculate:

(7)

$$J_{1cm^2} = \max\{\frac{1}{A}\iint_A J(r)dA\} = \frac{1}{1cm}\int_{14cm}^{15cm} J(r)dr = 6.58\frac{\mu A}{m^2}$$

(8)

$$SAR_{10_g} = \max\{\frac{1}{V}\iiint_V SAR(r)dV\} = \frac{1}{\sqrt[3]{10}cm}\int_{15-\sqrt[3]{10}}^{15} SAR(r)dr = 0.174\frac{pW}{kg}$$

(9)

$$SAR_{wb} = \frac{\sigma(\pi f r_0 H)^2}{2\rho} = 0.1007\frac{pW}{g}$$

where $J_{1cm}{}^2$ is current density averaged to 1cm^2, SAR_{10g} – Specific Absorption Rate averaged to 10 g and SAR_{wb} is whole body SAR.

After that the numerical calculations have been done to validate the algorithm. The results can be seen in Fig. 2 – Fig. 4.

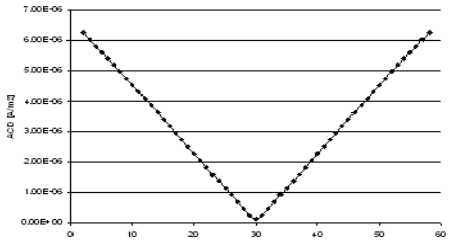

Fig. 2. The variation of ACD over disk radius.

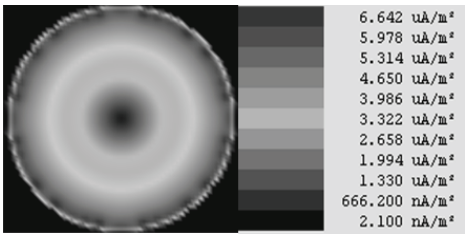

Fig. 3. ACD @ 50 Hz

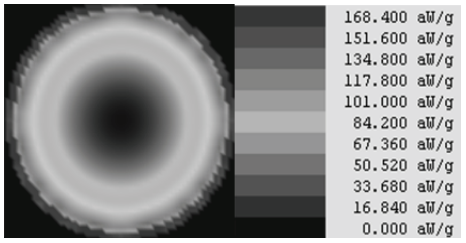

Fig. 4. SAR @ 50 Hz

Model of female breast phantom

The above algorithm has been applied to numerically investigate SAR and ACD distributions in a female breast model as it is shown in Fig. 5.

The details of the phantom preparation and its use in hyperthermia set can be found in [6]. In real low frequency hyperthermia sets, a working frequency of applicator can vary. In our case the frequency was in the range from 140 to 160 kHz. That is why ACD and SAR dependence on frequency in the skin and cancer layer have been investigated.

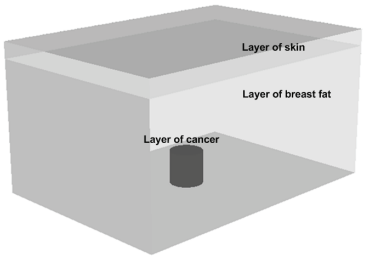

Fig. 5. CAD model of female breast phantom

The dielectric parameters of the modeled tissues have been approximated using 4-Cole-Cole [7] with parameters taken from Gabriels [8] and calculated for frequencies: 140, 150 and 160 kHz (see Table 1)

Table 1. The dielectric parameters of the model

Tissue	σ [S/m]	ρ [g/cm^3]
Skin	0.089014 @ 140 kHz 0.093995 @ 150 kHz 0.09869 @ 160 kHz	1.01
Breast fat	0.025111 @ 140 kHz 0.025124 @ 150 kHz 0.025137 @ 160 kHz	0.92
Cancer (Muscle)	0.37043 @ 140 kHz 0.37265 @ 150 kHz 0.37491 @ 160 kHz	1.04

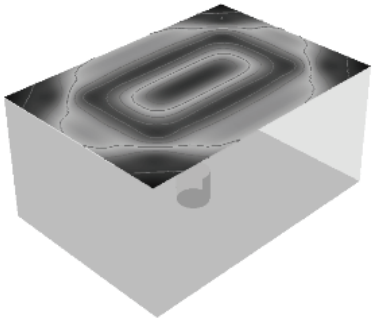

Fig. 6. ACD @ 140kHz – skin layer.

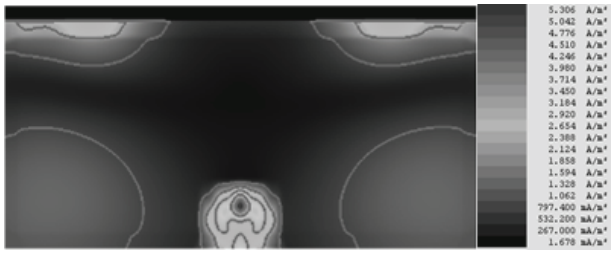

Fig. 7. ACD @ 140kHz – vertical cross section of the phantom.

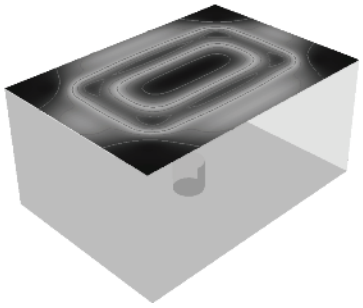

Fig. 8. SAR_{1g} @ 140 kHz – skin layer

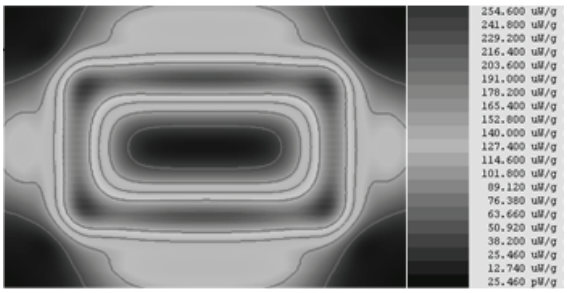

Fig. 9. SAR_{1g} @ 140 kHz - vertical cross section of the phantom

Table 2. Maximum values of ACD and SAR in the skin

f [kHz]	max ACD [A/m^2] skin	SAR_{1g} [μW/g] skin
140	3.126	254.6
150	3.604	337.8
160	4.162	435.6

Table 3. Frequency dependence of maxACD and SAR in the cancer

f [kHz]	maxACD [mA/m^2]	SAR_{avg} [pW/g]
140	7.37	304.2
150	8.214	368.8
160	9.312	440.4

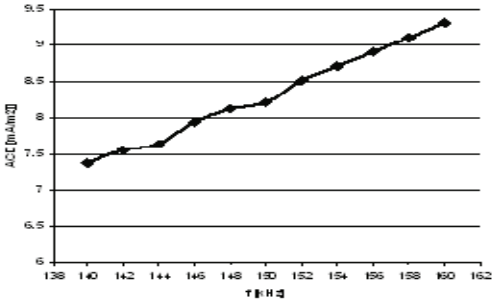

Fig. 10. Frequency dependence of ACD

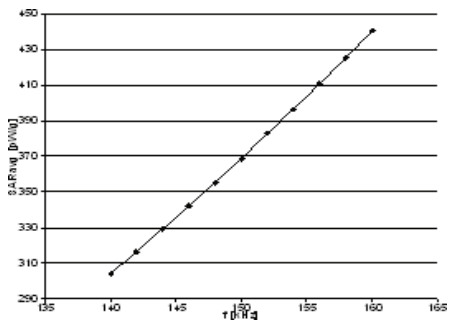

Fig. 11. Frequency dependence of SARavg

In the pictures (Fig. 6 – Fig. 8) are shown the exemplary SAR and ACD distributions in the model for the frequency of 140 kHz. The results of calculations for different frequencies are gathered in Table 2.

As it can be seen from Fig. 6 – Fig. 9, the highest value of ADCs and SARs have occurred in the cancer and skin layers. The results of frequency dependence of alternating current density averaged to 1cm^2 together with average SAR are gathered in Table 3. Moreover, in graphs (see Fig. 10-11) the linear nautre of the considered phenomenon can be observed.

Conclusions

The value of magnetic field strength used in the analysis has been chosen arbitrarily (H = 1 A/m), as the problem is of linear nature. Thus, the results of calculation can be re-scaled to the magnetic field as one wishes. Eddy currents and SAR are of great importance when talking about inductive heating. The maximum ACD and SAR values in the body are determined by the size of the body, and so is the distance between the applicator and the skin. Nevertheless, the knowledge of them plays an important role when skin overheating is taken into consideration. The authors hope that the presented results can help to design inductive hyperthermia applicators and avoid the skin overheating problem.

REFERENCES

[1] Gas P., Temperature inside tumor as time function in RF hyperthermia, *Electrical Review*, (2010), No. 12, 42–45.

[2] Taflove A., Computaional Electrodynamics The Finite-Difference Time-Domain Method, (1995), Artech House.

[3] Miaskowski A., Krawczyk A., Wac-Włodarczyk A, The investigation of electromagnetic field influence generated by mobile phones on cardiac pacemakers with the anatomically based human model, *COMPEL: The International Journal for Computation and Mathematics in Electrical and Electronic Engineering*, (2008), Vol. 27 No. 4, 728-734.

[4] Miaskowski A., Krawczyk A., Finite Difference Time Domain Method for High Resolution Modeling of Low Frequency Electric Induction in Humans, *Electrical Review,* (2007), No. 11, 225-227.

[5] Berenger J., A perfectly matched layer for the absorption of electromagnetic waves, *Journal of Computational Physics* 114: 1994, pp. 185–200

[6] Miaskowski A., Sawicki B., Krawczyk A., Yamada S., The application of magnetic fluid hyperthermia to breast cancer treatment, *Electrical Review,* (2010), No. 12, 99-101

[7] Cole K.S., Cole R.H., *Dispersion and absorption in dielectrics*: *I. Alternating current characteristics*, Journal of Chemical Physics, (1941), 341-351.

[8] Gabriel S., Lau R.W., Gabriel C., The dielectric properties of biological tissues: III. Parametric models for the dielectric spectrum of tissues, *Phys. Med. Biol.*,(1996), No. 41, 2271-2293

***Authors**: dr inż. Arkadiusz Miaskowski, University of Life Sciences in Lublin, Department of Applied Mathematics and Computer Science, Akademicka 13, 20-950 Lublin, E-mail: arek.miaskowski@up.lublin.pl; dr hab. inż. Andrzej Wac-Włodarczyk, Lublin University of Technology, Institute of Electrical Engineering and Electrotechnologies, Nadbystrzycka 38a, 20-618 Lublin, E-mail: a.wac-wlodarczyk@pollub.pl, dr hab. n. med. Grażyna Olchowik, Medical University of Lublin, Department of Biophysics, Jaczewskiego 4, 20-090 Lublin, E-mail: grazyna.olchowik@am.lublin.pl*